

# Can a conditioning on stellar mass explain the mutual information between morphology and environment?

Snehasish Bhattacharjee,<sup>a,1</sup> Biswajit Pandey,<sup>b</sup> Suman Sarkar<sup>b</sup>

<sup>a</sup>Department of Astronomy, Osmania University, Hyderabad, 500007, India

<sup>b</sup>Department of Physics, Visva-Bharati University, Santiniketan, 731235, India

E-mail: [snehasish.bhattacharjee.666@gmail.com](mailto:snehasish.bhattacharjee.666@gmail.com), [biswap@visva-bharati.ac.in](mailto:biswap@visva-bharati.ac.in),  
[suman2reach@gmail.com](mailto:suman2reach@gmail.com)

**Abstract.** Recent studies with SDSS have shown that a statistically significant non-zero mutual information between morphology and environment persists up to several tens of Mpc, which awaits an explanation. Galaxies in different environments acquire their stellar mass through accretion and merger and the stellar mass function of galaxies is known to depend on both environment and morphology. Naturally, stellar mass can be an important link between morphology and environment which may explain the non-zero mutual information between the two. Measuring the mutual information between morphology and environment by conditioning the stellar mass would allow us to test this possibility. We employ here a volume and stellar mass limited sample from the 16<sup>th</sup> data release (DR16) of the SDSS and find a non-zero conditional mutual information throughout the entire length scales probed. We compare the results with three different semi-analytic models implemented on the Millennium simulation and find their predictions to be in fairly good agreement with SDSS on smaller length scales ( $\lesssim 30 h^{-1}$  Mpc), with a clear discrepancy observed at larger length scales ( $\gtrsim 30 h^{-1}$  Mpc) where the models predict significantly lower conditional mutual information than the SDSS. Our analysis therefore suggests that only environmental and morphology dependence of stellar mass are inadequate in explaining the observed mutual information between morphology and environment and that physical processes which alters morphology may not necessarily have an impact on the stellar mass of galaxies and vice versa.

---

<sup>1</sup>Corresponding author.

---

## Contents

<b>1</b>	<b>Introduction</b>	<b>1</b>
<b>2</b>	<b>Methodology</b>	<b>3</b>
2.1	The Mutual Information between Morphology and Environment	4
2.2	The Mutual Information between Stellar Mass and Environment	5
2.3	The Conditional Mutual Information between Environment, Morphology and Stellar Mass	5
<b>3</b>	<b>Data</b>	<b>6</b>
3.1	The SDSS sample	6
3.2	The Millennium samples	6
<b>4</b>	<b>Results</b>	<b>7</b>
4.1	Significance of mutual information	7
4.2	MI and CMI: Comparing SDSS with SAM	9
<b>5</b>	<b>Conclusions</b>	<b>11</b>

---

## 1 Introduction

Understanding the formation and evolution of galaxies remains one of major goals of modern cosmology. Environment is known to play a governing role in the formation and evolution of galaxies. It is now well known that environment imparts a significant influence on different galaxy properties [1–10]. The massive ellipticals are found to reside in rich clusters and spirals predominantly belong to groups or fields [11–14]. This fact was further re-established using the two point correlation function in [15–17] where ellipticals were found to be clustered richly in contrast to spirals. In a study of the filamentarity of the galaxy distribution [18], spirals were found to be distributed sporadically in the filaments whereas ellipticals favored to reside densely in the nodes of the filament intersections.

The local density is the most widely used indicator for the environment of a galaxy. But the local density alone may not solely describe the environmental dependence of galaxy properties. The dark matter haloes assemble in a hierarchical fashion and the galaxies are believed to form later inside these haloes via radiative cooling and condensation of baryons [19]. In the halo model, the mass of a dark matter halo decides all the properties of the galaxy formed within it [20]. However the different assembly history of the dark matter haloes across the different parts of the cosmic web leads to different clustering for them which is known as the assembly bias [21–24]. The galaxies in the Universe are distributed along a vast interconnected network of sheets, filaments and clusters encompassing nearly empty regions in between them. The highly anisotropic nature of these structures lead to variations in mass, shape, size and spin of dark matter haloes residing in these large-scale environments [25]. So the large-scale cosmic environment may also play a significant role in the galaxy formation and evolution.

A number of observations indicate that there are significant correlation between the galaxy properties and their large-scale environment. Employing data from SDSS, Scudder

[26] report substantial difference in the star formation rates between groups embedded in high density superclusters and the groups residing in isolation. Using data from SDSS, Luparello [27] report strong dependence between properties of late type brightest group galaxies and their large scale environment. An analysis of the filamentarity of the galaxy distribution using SDSS by Pandey & Bharadwaj [28] reveal that average filamentarity of the red galaxies are significantly lower than the starburst galaxies. Darvish [29] report that the presence of filamentary environment increases the fraction of starburst galaxies at  $z \sim 1$ . An analysis of the galaxies in SDSS by Filho [30] reveal that almost three quarters of the most extremely metal poor galaxies are embedded in voids and sheets. A recent work by Pandey & Sarkar [31] find that the fraction of red galaxies in filaments and sheets increases with the size of these structures. Park [32] analyzed galaxies from SDSS and find weak dependency between large scale environment and galaxy properties once the contributions of morphology and luminosity are accounted for. Yan [33] employed data from SDSS and report that the tidal environment of the large scale structures has no influence on the galaxy properties.

Pandey & Sarkar [34] analyzed the data from SDSS and report that morphology and environment share a non-zero mutual information (hereafter MI) which decreases with increasing length scales. A recent analysis by Sarkar & Pandey [35] show that these MI are statistically significant at 99.9% confidence level throughout the entire length scale probed. In the present work, we would like to understand the physical origin of such non-zero MI which persists up to such large length scales.

The integrated stellar mass of a galaxy is thought to be the most fundamental property which largely influences its structure and evolution [36]. It is often taken as an impression of its formation history and governs its future evolution [36]. Galaxies assemble gas through both mergers and as well as various secular processes [37, 38]. This gas upon condensation, give rise to molecular clouds which in turn become stellar nurseries. Hence, high stellar mass represent more evolved systems. Furthermore, stellar mass of a galaxy correlate with other galactic properties, such as star formation rate, metallicity and halo mass [39–44]. Thus, different scaling relations involving stellar mass coupled with the galaxy stellar mass function (GSMF), are hypothesized to pose salient constraints for the formation and evolutionary models of galaxies [45, 46].

We investigate if the stellar mass which is linked to both morphology and environment contributes to the non-zero MI between morphology and environment. Although the stellar mass function of galaxies is reported to be similar in clusters and field up to  $z \sim 1.5$  [74–76, 78], it is not the case when the environment is parametrized by the local number density. Under these presumptions the stellar mass function is reported to vary with environment [47, 48]. These variations can be partly explained by halo biasing [49, 50]. However biasing can not provide a complete understanding of the connection between galaxy and dark matter halo. Besides, the stellar mass function of galaxies is also known to be sensitive to their morphology [51]. Denser regions are preferentially inhabited by high mass haloes which are again mostly populated by high stellar mass galaxies with early-type morphology [52]. There is a fair possibility that the observed MI between morphology and environment is a consequence of these relations. Bamford [52] studied the environmental dependence of morphology using the Galaxy Zoo [53] data and found that morphology exhibits very weak environmental trends once the stellar mass is fixed. We would like to understand the role of stellar mass on the observed environmental dependence of morphology using an information theoretic perspective [34]. The present manuscript aims to investigate whether environmental dependence and morphology dependence of stellar mass of a galaxy can explain the observed MI between

environment and morphology [34].

It is also important to verify the observational findings with the current models of galaxy formation and evolution. Semi analytic models of galaxy formation and evolution (SAM) are prevailing tools for understanding the hierarchical growth of dark matter haloes and temporal evolution of galaxies within [54–56]. Distinguishable from empirical abundance matching [57, 58] or halo occupation distribution models [59], SAMs utilize a forward-modeling approach and are designed such that it include sufficient baryonic physics required for understanding galaxy evolution, although at a much simplified and macroscopic level [60]. This macroscopic nature of SAM make them computationally inexpensive compared to hydrodynamical simulations. However, predictions of SAMs need to be confirmed by observations to understand their efficiency and applicability. We analyze observational data from the 16<sup>th</sup> data release (DR16) of the SDSS and compare the results against SAMs implemented on the Millennium simulation.

The paper is organized as follows: In Section II we describe the methodology, in Section III we delineate the method of analysis. In Section IV we describe the data used in the paper, in Section V we discuss the results and in Section VI we present our conclusion.

Throughout this work, we calculate the comoving distances from redshifts using the flat  $\Lambda$ CDM model with  $\Omega_m = 0.315$ ,  $\Omega_\Lambda = 0.685$  and  $h = 0.674$  [68].

## 2 Methodology

In this work we are interested in investigating whether only environmental and morphology dependence of stellar mass are inadequate in explaining the observed MI between morphology and environment. For the purpose of analysis we use the method proposed in Pandey & Sarkar [34]. A brief description of the method is as follows. We construct a sample comprising  $\Psi$  number of galaxies within a cubic region. The galaxies belong to two distinct populations which we represent by "population A" and "population B". We proceed to divide the cube into regular square grids each having a volume of  $(d h^{-1} \text{ Mpc})^3$ . Thus the cube is now fractionated into many smaller cubic voxels each of sidelength  $d h^{-1} \text{ Mpc}$ . Let  $\Phi_d$  be the number of the cubic voxels for a fixed grid size of  $d$  resulted after fractionating the bigger cube. The aim here is to count the number of population A and population B galaxies in each voxel. Let  $(\psi_A)_i$  and  $(\psi_B)_i$  be the number of population A and population B galaxies settling in the  $i^{\text{th}}$  voxel respectively. Therefore,  $\psi_i = (\psi_A)_i + (\psi_B)_i$  is the total number of galaxies located in the  $i^{\text{th}}$  voxel. Summing over all the  $\Phi_d$  voxels yields  $\sum_{i=1}^{\Phi_d} (\psi_A)_i = \psi_A$ ,  $\sum_{i=1}^{\Phi_d} (\psi_B)_i = \psi_B$  and  $\sum_{i=1}^{\Phi_d} (\psi_i)_i = \Psi$ , where  $\psi_A$ ,  $\psi_B$  and  $\Psi = \psi_A + \psi_B$  are the total number of population A, population B and total number of galaxies in the sample respectively. We proceed to define two discrete random variables  $X$  and  $Y$  with respective probability distributions  $P(X)$  and  $P(Y)$ , where  $P(X_i) = \frac{\psi_i}{\Psi}$  represents the probability of a galaxy chosen at random settles in the  $i^{\text{th}}$  voxel and  $P(Y)$  is the probability of a galaxy chosen at random is either a population A or a population B galaxy. Clearly  $P(X)$  has  $\Phi_d$  number of possibilities while  $P(Y)$  has only two and is given by  $P(Y_1) = \frac{\psi_A}{\Psi}$  for population A and  $P(Y_2) = \frac{\psi_B}{\Psi}$  for population B. We vary the grid size  $d$  and compute  $P(X)$  in each case. We note that  $P(Y)$  is insensitive to the grid size and remain constant throughout the analysis. The total number of galaxies within each voxel changes as the grid size  $d$  is changed but the total number of galaxies within the cube is constant. We compute a set of information theoretic measures based on the counts in these voxels.

## 2.1 The Mutual Information between Morphology and Environment

In information theory, the average amount of information necessary to explain a random variable  $x$  is called the information entropy  $H(x)$  and reads [61]

$$H(x) = - \sum_{i=1}^n p(x_i) \log p(x_i) \quad (2.1)$$

where  $p(x_i)$  denote the probability of the  $i^{th}$  outcome and  $n$  is the total number of outcomes. We set the base of the logarithm to be 10 throughout the analysis.

We have two variables  $X$  and  $Y$  defined for the environment on scale  $d$  and morphology respectively. We would like to measure the association between these two random variables on different length scales  $d$ . The joint entropy  $H(X, Y)$  for the two random variables  $X$  and  $Y$  in this case would be,

$$H(X, Y) = - \sum_{i=1}^{\Phi_d} \sum_{j=1}^2 P(X_i, Y_j) \log P(X_i, Y_j) \quad (2.2)$$

where  $P(X, Y)$  is the joint probability distribution for  $X$  and  $Y$ . The joint probability  $P(X, Y)$  that a galaxy of a particular morphology (population A or population B) chosen at random settles in the  $i^{th}$  voxel reads

$$P(X, Y) = P(Y|X)P(X) \quad (2.3)$$

where  $P(Y|X)$  is the conditional probability of a galaxy chosen at random is either population A or population B given that it settles in the  $i^{th}$  voxel. Finally, the MI  $I(X; Y)$  between  $X$  and  $Y$  is given as [63]

$$\begin{aligned} I(X; Y) &= \sum_{i=1}^{\Phi_d} \sum_{j=1}^2 P(X_i, Y_j) \log \frac{P(X_i, Y_j)}{P(X_i)P(Y_j)} \\ &= H(X) + H(Y) - H(X, Y) \end{aligned} \quad (2.4)$$

$I(X; Y) \geq 0$  as  $H(X) + H(Y) \geq H(X, Y)$  with equality only when  $X$  and  $Y$  are independent. We compute  $I(X; Y)$  on different length scales by varying the grid size  $d$ .

The MI quantifies the expected gain in information on one variable given that the other one is observed. In the framework of information theory, this implies the reduction in uncertainty in estimating one variable given the knowledge of the other. A high value of  $I(X; Y)$  indicates that both the random variables depend strongly on each other and therefore corresponds to a large reduction in uncertainty and vice versa. One particular advantage offered by MI is that it does not assume the nature of relationship between the two random variables and hence is sensitive to both linear and non-linear correlations.

It can be also expressed as a Kullback-Leibler (KL) divergence [62] or relative entropy which is the difference between cross entropy and entropy. When the true distribution A is unknown, one may choose another distribution B as a model that approximates A. The cross-entropy is thus defined as  $H(A, B) = - \sum_i A_i \log B_i$  and KL divergence is defined as,  $KL(A||B) = \sum_i A_i \log \frac{A_i}{B_i}$ . So the mutual information can be defined as the following KL divergence,

$$\begin{aligned} I(X; Y) &= \sum_i \sum_j P(X_i, Y_j) \log \frac{P(X_i, Y_j)}{P(X_i)P(Y_j)} \\ &= KL(P(X, Y)||P(X)P(Y)) \end{aligned} \quad (2.5)$$

Thus the mutual information can be also considered as the error of using  $P(X)P(Y)$  to model the joint probability  $P(X, Y)$ . When  $X$  and  $Y$  are independent of each other i.e.  $P(X, Y) = P(X)P(Y)$  then their mutual information is zero.

## 2.2 The Mutual Information between Stellar Mass and Environment

We now define another random variable  $Z$  which characterizes the stellar mass of the galaxies. Similar to the previous section, the MI  $I(X; Z)$  between environment and stellar mass is defined as,

$$\begin{aligned} I(X; Z) &= \sum_{i=1}^{\Phi_d} \sum_{k=1}^2 P(X_i, Z_k) \log \frac{P(X_i, Z_k)}{P(X_i)P(Z_k)} \\ &= H(X) + H(Z) - H(X, Z) \end{aligned} \quad (2.6)$$

where  $k = 1$  for low stellar mass galaxies and  $k = 2$  for high stellar mass galaxies. In this work we treat galaxies having mass higher or equal to the median stellar mass of the sample as being high mass galaxies and vice versa. The joint entropy for environment and stellar mass is given as

$$H(X, Z) = - \sum_{i=1}^{\Phi_d} \sum_{k=1}^2 P(X_i, Z_k) \log P(X_i, Z_k) \quad (2.7)$$

## 2.3 The Conditional Mutual Information between Environment, Morphology and Stellar Mass

The positive MI between morphology and environment does not by definition mean a causal dependence between these galactic properties. The MI between environment and morphology may come from the shared MI between stellar mass, environment and morphology. To investigate this, we shall define the conditional mutual information (hereafter CMI) between between stellar mass, morphology and environment.

The CMI [64] furnish the expected value of the MI between two random variables given that we have complete knowledge of a third random variable. In this work, we are investigating the MI between morphology and environment of the galaxies given the knowledge of their stellar masses.

The CMI between  $X$  and  $Y$  for a given  $Z$  reads,

$$\begin{aligned} I(X; Y|Z) &= \sum_{i=1}^{\Phi_d} \sum_{j=1}^2 \sum_{k=1}^2 P(X_i, Y_j, Z_k) \log \frac{P(X_i)P(Y_j, Z_k)}{P(X_i, Z_k)P(Y_j, Z_k)} \\ &= H(X, Z) + H(Y, Z) - H(X, Y, Z) - H(Z) \end{aligned} \quad (2.8)$$

where  $H(X, Y, Z)$  is the joint entropy for the three random variables. The joint entropy  $H(X, Y, Z)$  is defined as,

$$H(X, Y, Z) = - \sum_{i=1}^{\Phi_d} \sum_{j=1}^2 \sum_{k=1}^2 P(X_i, Y_j, Z_k) \log P(X_i, Y_j, Z_k) \quad (2.9)$$

The joint probability denoted by  $P(X_i, Y_j, Z_k) = P(Z_k|Y_j, X_i)P(Y_j|X_i)P(X_i)$  can be estimated by counting the galaxies of different morphology and stellar mass in  $\Phi_d$  different voxels within the datacube.

The CMI  $I(X; Y|Z) \geq 0$  with equality only when the information shared between  $X$  and  $Y$  is just a byproduct of the information contained about these variables in  $Z$ . In other words,  $I(X; Y|Z) = 0$  implies that  $X$  is independent of  $Y$  given the knowledge of  $Z$ . We vary the grid size  $d$  and compute  $I(X; Y|Z)$  corresponding to each length scale.

### 3 Data

#### 3.1 The SDSS sample

We use data from the 16<sup>th</sup> data release [65] of Sloan Digital sky survey (SDSS) for the present analysis. SDSS is presently the largest redshift survey which has mapped more than one third of the celestial sphere. The data is downloaded from the SDSS SkyServer<sup>1</sup> using structured query language. The *SpecPhotoAll* and *Photoz* tables of SDSS database are used to get the spectroscopic and photometric information of the galaxies. We look for a region devoid of any holes or patches so we select the contiguous region of the sky within  $0^\circ \leq \delta \leq 60^\circ$  and  $135^\circ \leq \alpha \leq 225^\circ$ ,  $\alpha$  and  $\delta$  respectively being the right ascension and declination of a galaxy. We select the galaxies within the  $r$ -band Petrosian apparent magnitude ( $r_p$ ) limit  $r_p < 17.77$ . We obtain the morphology of the galaxies from the *ZooSpec* table of DR16 database. This table holds morphological classification for SDSS galaxies provided through the Galaxy Zoo project<sup>2</sup>. In Galaxy Zoo [53, 66] millions of registered volunteers take part in visual classification of the galaxies. We note that in the present analysis population A galaxies represent ellipticals and population B galaxies represent spirals. We consider only the classified galaxies which are flagged as *spiral* or *elliptical* with a debiased vote fraction  $> 0.8$ . The galaxies which are flagged as *uncertain* are discarded from the present analysis. We obtain the stellar mass of galaxies from the *stellarMassFSPSGranWideNoDust* table. The stellar mass of SDSS galaxies provided in this table are calculated using the Flexible Stellar Population Synthesis (FSPS) techniques [67]. Combining these four tables from the SDSS database, we get a total 136108 galaxies up to redshift  $z < 0.3$ . We use these galaxies to prepare a volume limited sample with  $r$ -band absolute magnitude limit  $M_r \leq -21$ , stellar mass range  $1 \times 10^{10} M_\odot \leq M_* \leq 6 \times 10^{11} M_\odot$  and redshift range  $z \leq 0.115$ . The median mass of the sample is  $\simeq 8.054 \times 10^{11} M_\odot$ . The resulting volume and mass limited sample contains a total of 43092 galaxies. However, the present analysis requires a cubic region. The largest cube that we are able to extract from the volume limited sample has a side length of  $174 h^{-1} \text{ Mpc}$ . There are in total 15373 galaxies within the cube. 11481 of them are spirals and 3892 are ellipticals.

#### 3.2 The Millennium samples

The Millennium Simulation is a cosmological simulation<sup>3</sup> carried out by the Virgo Consortium<sup>4</sup> and described in detail in [69]. The simulation tracks  $2160^3$  particles each of mass  $8.6 \times 10^8 h^{-1} M_\odot$  enclosed in a comoving box of size  $500 h^{-1} \text{ Mpc}$  on a side and assumes  $\Lambda\text{CDM}$  cosmology with cosmological parameters  $\Omega_m = 0.25$ ,  $\Omega_b = 0.045$ ,  $h = 0.73$ ,  $\Omega_\Lambda = 0.75$ ,  $n = 1$ ,

<sup>1</sup><https://skyserver.sdss.org/casjobs/>

<sup>2</sup><http://zoo1.galaxyzoo.org>

<sup>3</sup> <http://www.mpa-garching.mpg.de/galform/virgo/millennium/>

<sup>4</sup> <http://www.virgo.dur.ac.uk/>



$\sigma_8 = 0.9$ . Since it is not practically feasible to analyze the large number of SAMs available in literature in one study, we shall therefore use the data of only 3 SAMs implemented on the Millennium Simulations. We analyze here for representative purposes the SAMs published by S. Bertone et al [70] (hereafter B2007), Q. Guo et al [71] (hereafter G2013) and by B.M.B Henriques et al [72] (hereafter H2020). A brief description of the SAMs are as follows: The B2007 model [70] presents an enhanced feedback scheme constructed upon a dynamical treatment of the evolution of galactic winds replacing the previous use of supernova feedback without altering the AGN feedback and with recycling and ejection of gas and metals being treated self-consistently governed by the dynamical evolution of winds. The G2013 model [71] investigates how the growth of structures vary with cosmological parameters derived from WMAP1 & WMAP7 by scaling the Millennium and Millennium II simulations using the re-scaling technique developed by Angulo & White [77]. Finally, the H2020 model [72] is a recently published spatially resolved model of cold gas partitioning, star formation, mass and elements feedback and observationally consistent global properties which is argued to offer new opportunities to interpret the results on ongoing galaxy surveys. We download the data from the Millennium database <sup>5</sup> using a Structured Query Language (SQL) search. We extract the position coordinates, peculiar velocities, bulge mass and total stellar masses of all the galaxies with  $r$ -band absolute magnitude limit  $M_r \leq -21$  and stellar mass range  $1 \times 10^{10} M_\odot \leq M_* \leq 6 \times 10^{11} M_\odot$ . We carve out 8 non-overlapping cubic regions of side  $174 h^{-1}$  Mpc from each of the SAM catalogues. Note that the simulated galaxies are in real space whereas the observed galaxies are in redshift space. Hence, for a fair analysis, we map the 3D comoving coordinates of the simulated galaxies in redshift space employing their peculiar velocities. As the morphology of the galaxies are not directly available, we divide the mass of the bulge  $M_{bulge}$  to the stellar mass  $M_{stellar}$  (i.e,  $\frac{M_{bulge}}{M_{stellar}} = \Theta$ ) for each galaxy and use this parameter as a proxy for morphology. Since ellipticals are mostly bulge dominated, we define all galaxies with  $\Theta \geq 0.8$  as ellipticals. Spirals are known to have a relatively smaller bulge component. We define spirals as galaxies with  $\Theta \leq 0.4$ . We discard all simulated galaxies with  $0.4 < \Theta < 0.8$ . This ensures that the selected galaxies are primarily of two types - bulge dominated and disk dominated. We randomly extract 15373 galaxies from each of these distributions in redshift space keeping the same ratio of spirals to ellipticals. Finally for each SAM, we end up with 8 cubes with side length  $174 h^{-1}$  Mpc. Each of these datacube host 11481 spiral galaxies and 3892 elliptical galaxies. We show the distribution of stellar mass in the galaxy samples from the SAMs in Fig. 1. The result for the SDSS sample is also shown together for a comparison. The mock datacubes from the SAMs are analyzed exactly the same way as the SDSS data.

## 4 Results

### 4.1 Significance of mutual information

In order to understand the connection between environment ( $X$ ) and morphology ( $Y$ ), we calculate the MI  $I(X; Y)$  between these quantities for the SDSS sample.

We have restricted our analysis to the minimum length scale of  $\sim 14 h^{-1}$  Mpc as the mean intergalactic separation of our samples were of the order of  $10 h^{-1}$  Mpc. A further decrease in the lengths of the voxels would result in an increase in the amplitude of fluctuations and therefore would yield spurious results. Additionally, note that the maximum length scale

<sup>5</sup><http://gavo.mpa-garching.mpg.de/Millennium/>



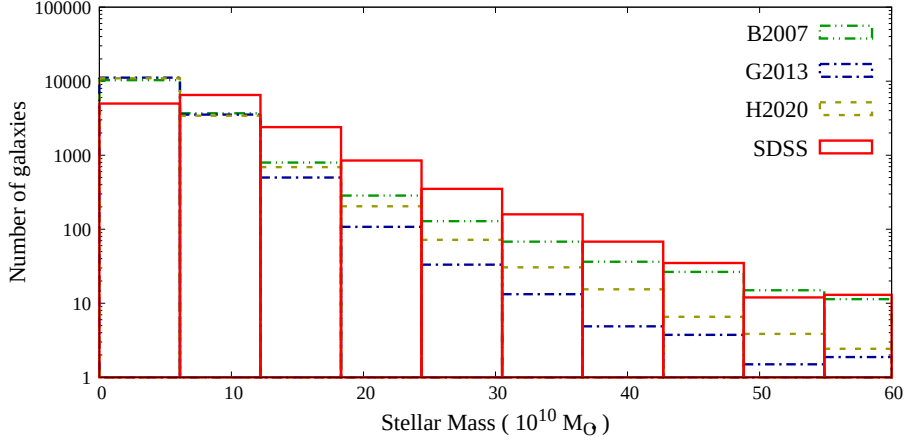


**Figure 1.** This shows the number of galaxies as a function of stellar mass for the SDSS datacube and the mock datacubes from the SAMs. The number of galaxies in different stellar mass bins for the SAMs are averaged over 8 respective subcubes.

probed in this work is  $87 h^{-1}$  Mpc since the size of our data cube is  $174 h^{-1}$  Mpc, therefore the maximum size of a voxel can only be  $87 h^{-1}$  Mpc.

We find a positive MI between these quantities which decreases with increasing length-scale similar to the results obtained in [34]. This indicates that environment do influence morphology of any given galaxy and the degree of association decreases on larger scales. However, it is important to test the physical significance of any non-zero MI observed between environment and a galaxy property. To test the physical significance of the MI between morphology and environment, we randomize the morphological information of galaxies without affecting their spatial distribution. We consider all the 15373 galaxies in the SDSS datacube and randomly tag 3892 galaxies as ellipticals ignoring their actual morphology. Rest of the galaxies in the SDSS datacube are labelled as spirals. We repeat this procedure for 10 times to generate 10 such SDSS datacubes with randomly assigned morphology. This procedure randomize the information contained in the morphology of galaxies keeping the galaxy distribution unchanged. The adopted randomization procedure would not alter  $H(X)$  and  $H(Y)$  but would only affect  $H(X, Y)$ . The value of  $H(X, Y)$  should ideally tend to  $H(X) + H(Y)$  after randomization of morphology. Any physical connection between morphology and environment is thus expected to be destroyed by the randomization of morphological classification.

The results for the SDSS data with original morphological classification and its randomized counterparts are shown in Fig. 2. We find a significant reduction in the MI between morphology and environment when galaxies are assigned a random morphology. However a smaller non-zero MI between morphology and environment still persists in the randomized data which may originate from the finite size of the data sample. We verify this by using a set of Poisson distributions. We analyze 10 mock Poisson datacubes each of which contain same number of randomly assigned spirals and ellipticals as the SDSS datacube. We find that the MI for the Poisson random distributions are nearly identical to the SDSS data with randomized morphological information. So the residual non-zero MI which survives after randomization of morphological information of SDSS galaxies purely arises due to the discrete and finite nature of the sample. A detailed analysis of the statistical significance of these differences along with some other tests in the present context are presented in a recent paper

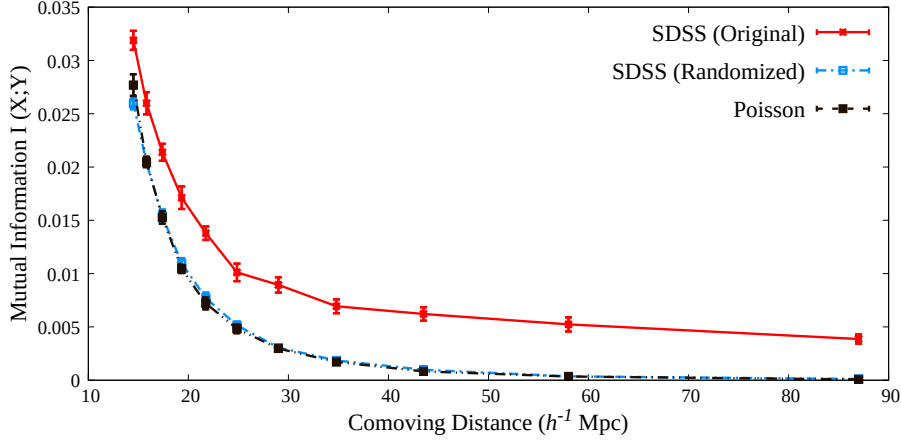


**Figure 2.** This shows the MI  $I(X;Y)$  between environment ( $X$ ) and morphology ( $Y$ ) for the original SDSS data and SDSS data with randomized morphological information. The error bars for the original SDSS data are obtained by bootstrap resampling whereas the error bars for the randomized dataset are obtained using 10 such realizations.

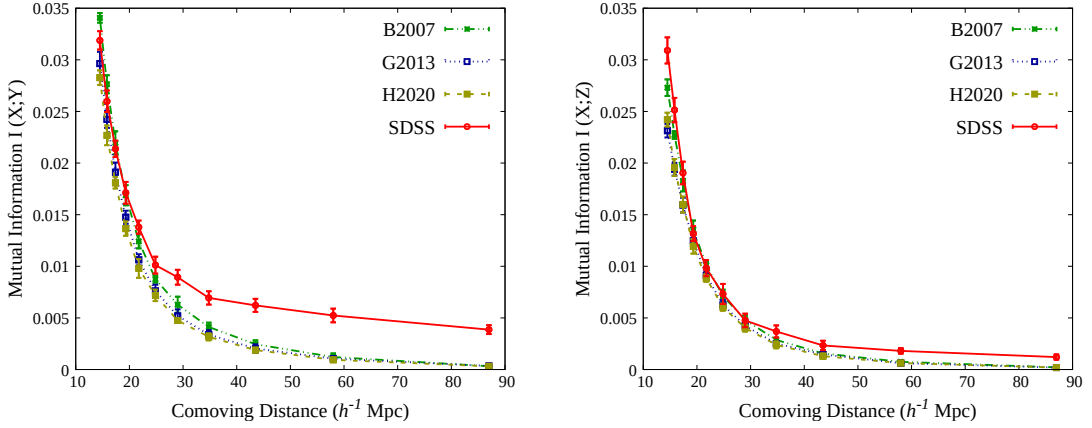


**Figure 3.** The left panel of this figure shows the MI  $I(X;Y)$  between environment ( $X$ ) and morphology ( $Y$ ) as a function of length scales while the right panel shows the MI  $I(X;Z)$  between environment ( $X$ ) and stellar mass ( $Z$ ) as a function of length scales for the SDSS and the semi analytical models. The error bars for the SDSS data are obtained by using 10 bootstrap samples whereas the error bars for the semi analytic models are derived using 8 subcubes drawn from each of the semi analytic catalogues.

[35].

Thus a part of the MI between morphology and environment must have some physical origin. The length-scale dependence of this MI may contain important information regarding the physical processes responsible for such correlations.

#### 4.2 MI and CMI: Comparing SDSS with SAM

In this section we investigate whether the MI between morphology and environment shown in Fig. 2 can be explained given a knowledge of stellar mass. This possibility arises due to the fact that stellar mass is correlated to both environment and morphology.

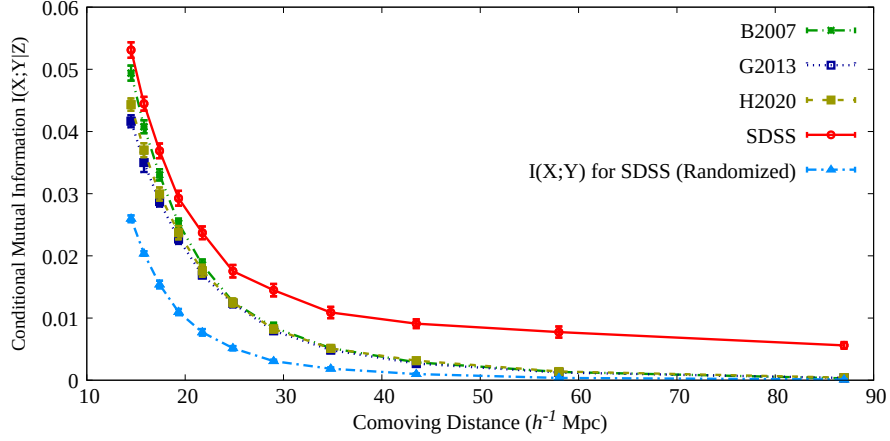


**Figure 4.** This shows the CMI  $I(X; Y|Z)$  between environment ( $X$ ), morphology ( $Y$ ) and stellar mass ( $Z$ ) as a function of length scales for the SDSS and the semi analytic models. The MI  $I(X; Y)$  between environment and morphology in the randomized SDSS data is shown together for a comparison. The error bars in each case are obtained in the same way as Fig. 2 and 3.

We first compare the MI between morphology and environment  $I(X; Y)$  in the SDSS with the SAMs considered. In the left panel of Fig. 3, we show  $I(X; Y)$  as a function of length scale for the SDSS and the SAMs. A positive MI between environment and morphology is observed for both the SDSS and the SAMs throughout the entire length-scale. The observed MI between environment and morphology in the SAMs show a fairly good agreement with SDSS on scales  $< 30 h^{-1}$  Mpc. However the MI between morphology and environment in the SDSS exhibit higher values compared to the SAMs on larger length scales ( $> 30 h^{-1}$  Mpc).

To carry out the analysis with stellar mass ( $Z$ ), we have divided the SDSS and SAM samples into two respective stellar mass bins. If the stellar mass of a galaxy is  $\leq 8.054 \times 10^{10} M_{\odot}$  (which is the median stellar mass of the SDSS sample) the galaxy resides in the lower stellar mass bin and otherwise in higher stellar mass bin. In the right panel of Fig. 3 we show the MI  $I(X; Z)$  between environment ( $X$ ) and stellar mass ( $Z$ ) for the SDSS and SAMs. We observe a positive MI between environment and stellar mass in the SDSS as shown in the Fig. 3. We find that the MI between stellar mass and environment in the SAMs agree fairly well with the SDSS observations. We observe some small differences in  $I(X; Z)$  between SDSS and SAMs at smaller ( $< 20 h^{-1}$  Mpc) and larger ( $> 40 h^{-1}$  Mpc) length scales.

A positive MI between environment and morphology can be a byproduct of the MI between environment and stellar mass. In other words, all the information morphology shares with environment can be explained from the knowledge of its stellar mass. To investigate this further, we compute the CMI between environment and morphology by conditioning the stellar mass (i.e,  $I(X; Y|Z)$ ) in Fig. 4. A perfect zero CMI would suffice the argument that stellar mass indeed is capable of explaining the MI between environment and morphology. However a perfect zero MI is not expected even in a randomized distribution or Poisson distribution where the two variables are known to be uncorrelated. We may recall that the MI  $I(X; Y)$  for the randomized SDSS data and the Poisson random distribution are identical at all length scales. So the MI between morphology and environment can be entirely explained by stellar mass only if the CMI turns out to be positive and equal to the MI expected for a Poisson random distribution.

The Fig. 4 shows that the CMI in SDSS is significantly higher than the MI  $I(X;Y)$  expected for the SDSS data with randomized morphological information. This implies that environmental and morphology dependence of stellar mass are not sufficient in explaining the correlation between morphology and environment at different length scales. The CMI predicted by the SAMs are also much higher as compared to the MI for random distributions. The CMI for both SDSS and SAMs are positive and larger than the non-zero MI expected from random distributions at all length scales which indicates that a part of the MI between morphology and environment may arise due to the associations of stellar mass with environment and morphology. However these correlations are unlikely to explain the entire MI between morphology and environment. We note that B2007 model predict a relatively higher MI and CMI than the G2013 and H2020 model on length scales  $< 30 h^{-1}$  Mpc. The three SAMs predict nearly the same MI and CMI on length scales  $> 30 h^{-1}$  Mpc. We find that the CMI measured in the SDSS is larger than the CMI predicted by the SAMs at all length scales. The results also indicate the existence of complex physical processes that alters the stellar mass or star formation of galaxies without affecting their morphologies and vice-versa. However, there is no general consensus as to what these processes are and therefore, future observations coupled with state-of-the art simulations should focus on answering this issue. It may be noted that the Mutual Information  $I(Y;Z)$  between morphology ( $Y$ ) and stellar mass ( $Z$ ) is not explored since  $I(Y;Z)$  is independent of length scale and therefore do not aid significantly in our investigation to understand how the correlations between two or more galactic properties vary with length scale.

## 5 Conclusions

In this paper we investigate the possibility that a prior knowledge of stellar mass of galaxies may explain the MI between environment and morphology. To investigate this, we employ an information theoretic framework developed in [34] to the publicly available SDSS DR16 and compare the results against semi analytic models implemented on the Millennium simulation.

We find a non zero MI between environment and morphology  $I(X;Y)$  for both SDSS and semi analytic models which indicates that morphology and environment are correlated up to several tens of Mpc. The MI between morphology and environment decreases with increasing length scales but remain non-zero throughout. We show that randomizing the information about the morphology of SDSS galaxies leads to a significant reduction in the MI between environment and morphology. This indicates that the randomization destroys the physical association between morphology and environment. We find a residual non-zero MI which is equal to that expected for a mock Poisson random distribution. This residual part of the non-zero MI originates from the finite and discrete nature of the distribution. However the excess part of the non-zero MI between morphology and environment owes an explanation. We investigate if this additional non-zero MI is a consequence of the fact that stellar mass is separately related to both morphology and environment.

We find a non-zero CMI between morphology, environment and stellar mass in the SDSS throughout the entire length scales probed. The observed CMI is significantly larger than the MI between morphology and environment expected in a randomized distribution with no existing correlation between the two. We conclude from the excess non-zero CMI that the environmental and morphological trends of stellar mass are inadequate in explaining the MI between morphology and environment. We compare these findings with three different semi-analytic models all of which predict significantly lower MI and CMI compared to SDSS

on larger length-scales. It is worthwhile to mention here that our analysis pertains to the local Universe only.

All three semi-analytic models (B2007, G2013, H2020) analyzed in this work, adopted a Chabrier initial mass function [79] in their modelling. The primary differences in the semi-analytic models lie in their choice of the cosmological parameters and the schemes for modelling various physical processes responsible for galaxy formation and evolution. The feedback processes (e.g. SNe feedback, AGN feedback) can significantly affect the growth of galaxies and shape their mass functions. Expulsion of gas from galaxies by SNe feedback drive the evolution of low mass galaxies, but do not significantly affect the evolution of high mass galaxies. The AGN feedbacks which are driven by the super-massive black holes (SMBH) at the centre of galaxies, suppress cooling in massive halos leading to a quenching in star formation. This turns the massive galaxies into “red and dead” ones which subsequently grow by mergers and become bulge dominated in the process. The choice of feedback schemes can thus indirectly affect the morphological mix of galaxies in different SAMs. The B2007 model used a new feedback scheme with a more efficient AGN feedback than those implemented in G2013 and H2020 models. The higher efficiency of the AGN feedback in the B2007 model is expected to produce a larger number of galaxies with higher stellar mass. This can be clearly seen in Fig. 1. The Fig. 1 also shows that the abundance of low stellar mass galaxies are nearly same in all the SAMs.

It is interesting to note that the MI and CMI (shown in Fig. 3 and Fig. 4) in the B2007 model show a somewhat better agreement with observations than the other two models on scales below  $30 h^{-1}$  Mpc. A more efficient AGN feedback in B2007 model yields a larger number of high stellar mass galaxies. The small-scale environments in the cosmic web may play an important role in the growth of the SMBHs in these galaxies [80] which are responsible for triggering AGN activities. The correlation between the environment and growth of SMBH may thus indirectly influence the mutual information between environment and galaxy properties such as morphology and stellar mass.

The MIs and CMIs in all the models are nearly identical on scales beyond  $30 h^{-1}$  Mpc. This indicates that the differences in the modelling of different physical processes and the associated parameters have hardly any influence on the measured MI and CMI on these length scales. The assembly bias [21–24] in simulations show that the early-forming low mass haloes are strongly clustered than the late-forming haloes of similar mass, which arises due to the differences in the accretion and merger histories of the haloes across different environments. The large-scale correlations observed both in SDSS and the models may be a consequence of the assembly bias which requires further studies. However, the discrepancy between the observed MI and CMI in SDSS and those predicted by different SAMs on scales beyond  $30 h^{-1}$  Mpc indicates that a better understanding of the role of large-scale environment is needed to account these differences.

Finally we note that morphology of galaxies are indeed correlated to their environment up to large length scales and we still lack a complete understanding of the physical origin of such large-scale correlations.

## Acknowledgments

The authors thank an anonymous reviewer for useful comments and suggestions which helped us to improve the draft. The authors would like to thank the SDSS team and the Galaxy

Zoo team for making the data public. The Millennium Simulation databases [73] used in this paper and the web application providing online access to them were constructed as part of the activities of the German Astrophysical Virtual Observatory (GAVO). BP acknowledges Steven P. Bamford for useful discussions. SB thanks Department of Science and Technology, New-Delhi, Government of India for the provisional INSPIRE fellowship selection [No:DST/INSPIRE/03/2019/003141]. BP would like to acknowledge financial support from the SERB, DST, Government of India through the project CRG/2019/001110. BP would also like to acknowledge IUCAA, Pune for providing support through associateship programme. SS would like to thank UGC, Government of India for providing financial support through a Rajiv Gandhi National Fellowship. SB and SS also thank Biswajit Das for discussions.

## References

- [1] M. Davis, & M. J. Geller, *ApJ*, **208**, 13 (1976).
- [2] L. Guzzo, M. A. Strauss, K. B. Fisher, R. Giovanelli, & M.P. Haynes, *ApJ*, **489**, 37 (1997).
- [3] I. Zehavi, et al., *ApJ*, **571**, 172 (2002).
- [4] T. Goto, C. Yamauchi, Y. Fujita, S. Okamura, M. Seikiguchi, I. Smail, M. Bernardi, P. L. Gomez, *MNRAS*, **346**, 601 (2003).
- [5] D. W. Hogg, et al., *ApJ Letters*, **585**, L5 (2003).
- [6] M. R. Blanton, et al., *ApJ*, **594**, 186 (2003).
- [7] J. Einasto, G. Hütsi, M. Einasto, E. Saar, , D. L. Tucker, V. Müller, P. Heinämäki, S. S. & Allam, *A&A*, **405**, 425 (2003).
- [8] G. Kauffmann, S. D. M. White, T. M. Heckman , et al., *MNRAS*, **353**, 713 (2004).
- [9] M. Mouhcine, I. K. Baldry, & S. P. Bamford, *MNRAS*, **382**, 80 (2007).
- [10] Y. Koyama, I. Smail, J. Kurk, et al., *MNRAS*, **434**, 423 (2013).
- [11] A. Oemler, *ApJ*, **194**, 1 (1974).
- [12] E. P. Hubble , *The Realm of the Nebulae* (Oxford University Press: Oxford), 79 (1936).
- [13] F. Zwicky, et al., 1961-1968, *Catalog of Galaxies and Clusters of Galaxies*, vols. 1-6 (Pasadena: California Institute of Technology)
- [14] A. Dressler, *ApJ*, **236**, 351 (1980).
- [15] C. N. A. Willmer, L. N. da Costa, & P. S. Pellegrini, *AJ*, **115**, 869 (1998).
- [16] M. J. I. Brown, R. L. Webster, & B. J. Boyle, *MNRAS*, **317**, 782 (2000).
- [17] I. Zehavi, et al., *ApJ*, **630**, 1 (2005).
- [18] B. Pandey & S. Bharadwaj, *MNRAS*, **372**, 827 (2006).
- [19] S. D. M. White & M. J. Rees, *MNRAS*, **183**, 341 (1978).
- [20] A. Cooray & R. K. Sheth, *Physics Reports*, **371**, 1 (2002).
- [21] L. Gao & S. D. M. White, *MNRAS*, **377**, L5 (2007).
- [22] M. Musso, C. Cadiou, C. Pichon, S. Codis, K. Kraljic, Y. Dubois, *MNRAS*, **476**, 4877 (2018).
- [23] M. Vakili & C. Hahn, *ApJ*, **872**, 115 (2019).
- [24] D. J. Croton, L. Gao, S. D. M. White, *MNRAS*, **374**, 1303 (2007).
- [25] O. Hahn, et al., *MNRAS*, **375**, 489 (2007).

- [26] J. M. Scudder, S. L. Ellison, & J. T. Mendel, MNRAS, **423**, 2690 (2012).
- [27] H. E. Luparello, et al., MNRAS, **448**, 1483 (2015).
- [28] B. Pandey & S. Bharadwaj, MNRAS, **387**, 767 (2008).
- [29] B. Darvish, et al., ApJ, **796**, 51 (2014).
- [30] M. E. Filho, et al., ApJ, **802**, 82 (2015).
- [31] B. Pandey & S. Sarakr, 2020, Submitted in MNRAS, arXiv:2002.08400
- [32] C. Park, & Y.-Y. Choi, ApJ, **691**, 1828 (2009).
- [33] H. Yan, Z. Fan, & S. D. M. White, MNRAS, **430**, 3432 (2013).
- [34] B. Pandey & S. Sarkar, MNRAS(L), **467**, 6 (2017).
- [35] S. Sarakr & B. Pandey, arXiv:2003.13974.
- [36] D. Wouter, et al., A& A, **624**, A102 (2019).
- [37] R. Sancisi, et al., The Astronomy and Astrophysics Review, **15**, 189 (2008).
- [38] R. S. Somerville, & R. Davé, ARA&A, **53**, 51 (2015).
- [39] J. Brinchmann, et al., MNRAS, **351**, 1151 (2004).
- [40] C. A. Tremonti, et al., ApJ, **613**, 898 (2004).
- [41] I. K. Baldry, K. Glazebrook, & S. P. Driver, MNRAS, **388**, 945 (2008).
- [42] M. A. Lara-López, et al., A&A, **521**, L53 (2010).
- [43] F. Mannucci, et al., MNRAS, **408**, 2115 (2010).
- [44] A. V. Kravtsov, A. A. Vikhlinin, & A. V. Meshcheryakov, Astronomy Letters, **44**, 8 (2018).
- [45] J. Schaye, et al., MNRAS, **446**, 521 (2015).
- [46] A. Pillepich, et al., MNRAS, **475**, 648 (2018).
- [47] M. L. Balogh, D. Christlein, A. I. Zabludoff, D. Zaritsky, ApJ, **557**, 117 (2001).
- [48] I. Zehavi, et al., ApJ, **571**, 172 (2002).
- [49] H. J. Mo & S. D. M. White, MNRAS, **336**, 112 (2002).
- [50] R. K. Sheth & G. Tormen, MNRAS, **308**, 119 (1999).
- [51] B. Vulcani, et al., MNRAS, **412**, 246 (2011).
- [52] S. P. Bamford, R. C. Nichol, I. K. Baldry, et al., MNRAS, **393**, 1324 (2009).
- [53] C. J. Lintott, et al, MNRAS, 389, 1179 (2008).
- [54] S. Cole, et al., MNRAS, **319**, 168 (2000).
- [55] R. S. Somerville, et al., MNRAS, **391**, 481 (2008b).
- [56] Q. Guo, et al., 2011, MNRAS, **413**, 101
- [57] C. Conroy , R. H. Wechsler, A. V. Kravtsov , ApJ, **647**, 201 (2006).
- [58] B. P. Moster, et al., ApJ, **710**, 903 (2010).
- [59] A. A. Berlind, D. H. Weinberg, ApJ, **575**, 587 (2002).
- [60] P. D. Mitchell, et al., MNRAS, **474**, 492. (2017).
- [61] C. E. Shannon, Bell System Technical Journal, 27, **379-423**, 623-656 (1948).
- [62] Kullback,S. & Leibler, R. A. , The Annals of Mathematical Statistics, **22**, 79 (1951)
- [63] C. B. Bell, Ann. Math. Statist., **33-2**, 587-595 (1962).



- [64] A. D. Wyner, *Information and Control*, **38-1**, 51-59 (1978).
- [65] R. Ahumada, et al., arXiv, arXiv:1912.02905
- [66] C. J. Lintott, et al, *MNRAS*, 410, 166 (2011).
- [67] C. Conroy, J. E. Gunn, M. White, *ApJ*, 699, 486 (2009).
- [68] Planck Collaboration, et al., 2018, arXiv, arXiv:1807.06209
- [69] V. Springel et al., *Nature*, **435**, 629 (2005).
- [70] S. Bertone, G. De Lucia, & P. A. Thomas, *MNRAS*, **379**, 1143 (2007).
- [71] Q., Guo, et al., *MNRAS*, **428**, 11 (2013).
- [72] B.M.B Henriques et al., *MNRAS*, **491**, 5795 (2020).
- [73] G. Lemson, the Virgo Consortium, arXiv, astro-ph/0608019 (2006).
- [74] B. Vulcani et al. *A&A*, **550**, A18 (2013).
- [75] R. Calvi et al. *MNRAS*, **432**, 11 (2013)
- [76] M. Annunziatella et al. *A&A*, **571**, 15 (2014).
- [77] R. E. Angulo, S. D. M. White, *MNRAS*, **405**, 143 (2010).
- [78] R. F. J. van der Burg et al., arXiv:2004.10757.
- [79] Chabrier G., *PASP*, **115**, 763 (2003)
- [80] Umehata H., Fumagalli M., Smail I., Matsuda Y., Swinbank A. M., Cantalupo S., Sykes C., et al., *Science*, **366**, 97 (2019)